PPPL-TRANS-133

STATISTICS OF POINCARÉ RECURRENCES AND THE STRUCTURE OF THE STOCHASTIC LAYER OF A NONLINEAR RESONANCE

Translated by:

N.M. Turitzin

FEBRUARY 1983

Translation of this work was supported by the U.S. Department of Energy Contract No. DE-AC02-76-CHO-3073. Reproduction, translation, publication, use and disposal, in whole or in part, by or for the United States Government is permitted.

PLASMA PHYSICS LABORATORY

PRINCETON UNIVERSITY

PRINCETON, NEW JERSEY

PREPARED FOR THE U.S. DEPARTMENT OF ENERGY, UNDER CONTRACT DE-AC02-76-CHO-3073.

Nuclear Physics Institute

CO AN USSR

Statistics of Poincaré Recurrences

and

The Structure of the Stochastic Layer of a Nonlinear Resonance

B.V. Chirikov and D.L. Shepelyansky

Institute of Nuclear Physics

Siberian Division

USSR Academy of Sciences

Novosibirsk 90, USSR

Preprint INP 81-69

Statistics of Poincaré Recurrences and The Structure of the Stochastic Layer of a Nonlinear Resonance

B.V. Chirikov and D.L. Shepelyansky

Presented at the IX International Conference of Nonlinear Oscillations (Kiev 1981)

Abstract

Motion in the stochastic layer around the separatrix of a nonlinear resonance was investigated. The integral distribution function $F(\tau)$ of trajectory recurrence times τ to the center of the layer was numerically determined. It was found that the distribution $F(\tau) = A\tau^{-p}$ is a power function, the exponent assuming two different values: for $\tau \ll \tau_0$, $p = 1/2$ and for $\tau \gg \tau_0$, $p = 3/2$ (time τ_0 is determined by the characteristics of the layer).

1. Introduction

Under broad assumptions the resonance of nonlinear oscillations in a Hamiltonian system can be described and studied in a pendulum approximation (see for example [1]):

$$H_r(P,\phi,t) = \frac{P^2}{2M} + \varepsilon V_r \cos\phi + \varepsilon V \left[\cos(\nu\phi - \theta) + \cos(\nu\phi + \theta)\right]. \qquad (1.1)$$

The first two terms of this Hamiltonian resonance describe an isolated nonlinear resonance, where the momentum P characterizes the deviation of unperturbed variable actions from their resonance values; the "mass" M is related to the nonlinearity of oscillations and is expressed by the derivative of the unperturbed frequency with respect to the action; ε is a small perturbation parameter, and V_r and ϕ are the amplitude and phase respectively of the resonant perturbation harmonic. The last term in (1.1) describes the interaction of a given resonance with the rest. To simplify the presentation, we will examine here the interaction of only with two resonances located symmetrically with respect to the basic resonance. The perturbation phase is $\theta = \Omega t + \theta_o$ and Ω characterizes the tuning away from the principal resonance; ν is an arbitary constant which, generally speaking, depends on the resonance geometry. We will assume in what follows that $M = V_r = 1$ and $\varepsilon V = \eta \sim \varepsilon << 1$. Under these conditions the frequency of phase oscillations at resonance $\Omega_\phi = \sqrt{\varepsilon}$. The basic small parameter of the resonance interaction is the relationship $\lambda^{-1} = \Omega_\phi/\Omega << 1$. The smallness of $1/\lambda$ indicates that resonances are well separated from one another.

The formal mathematical analysis of the "simple" system (1.1) encounters significant and still insurmountable difficulties, which were already known to Poincaré. Namely, the resonance interaction results in "splitting" of the unperturbed separatrix belonging to each of them and to the formation of a highly complex homoclinic structure. These difficulties can, however, be circumvented by constructing a roughly modified Poincaré mapping in $\phi = \pi$ plane (elliptical point of the basic resonance) [1]. For system (1.1), the mapping has the form:

$$\bar{w} = w + \xi \sin\theta; \quad \bar{\theta} = \theta + \lambda \ln \frac{32}{|\bar{w}|}, \tag{1.2}$$

where $w = H_r/\varepsilon - 1$ is the displacement with respect to the unperturbed separatrix θ is the perturbation phase in plane $\phi = \pi$ and

$$\xi = -2\pi \frac{\eta}{\varepsilon} \frac{(2\lambda)^{2\nu}}{\Gamma(2\nu)} \exp\left(-\frac{\pi}{2}\frac{\Omega}{\sqrt{\varepsilon}}\right) \tag{1.3}$$

is a new small perturbation parameter.

The mapping in the form (1.2) in addition to a general simplification of analytical and numerical study of the system (1.1) solves two important problems. First, it eliminates periodic perturbation effects, which cause only deformation but not separatrix splitting; for details see [1]. Second, a natural small parameter (1.3) appears, which can be used for asymptotic expansion and, in particular, it can be used quite effectively in an averaging

method [2]. Let us explain right away that an asymptotic expansion using the original minor parameter ε does not work because of the singularity of expression (1.3) for $\varepsilon \to 0$. In order to overcome this difficulty, which appeared at one time quite fundamental, it was found to be sufficient to integrate the equations of motion of the continuous system (1.1) exactly over a half period of phase oscillations rather than asymptotically. This was orginally done by Mel'nikov [3], who evaluated to within an order of magnitude the splintering of the separatrix produced by the small parameter ξ (1.3).

Introducing a new variable $y = w/\xi$ and neglecting the constant phase shift θ, we can write the mapping (1.2) as

$$\bar{y} = y + \sin\theta;\ \bar{\theta} = \theta - \lambda \ln |\bar{y}| \ . \qquad (1.4)$$

This canonical mapping, depending on a single parameter $\lambda >> 1$ will be investigated below.

2. Width of a Stochastic Layer

The most important characteristic of a homoclinical structure near the separatrix of a nonlinear resonance is its total width. Because of the very complex nature of this structure, a strict assessment of its width has not been successfully made up to now. In what follows we will briefly present an approximate solution of this problem [1] by linearization of the mapping (1.4) in y and reducing it to the so-called standard mapping

$$\bar{P} = P + K \sin\theta;\ \bar{\theta} = \theta + \bar{P}\ , \tag{2.1}$$

where $K = \lambda/y_r$ is a parameter characterizing, in our case, the local structure of the stochastic layer in the neighborhood $y = y_r$ of the resonance $\lambda \ln y_r = 2\pi r$ (r an integer) and $P = \lambda\,(y - y_r)/y_r$ is the new momentum.

The dynamics of the standard mapping (2.1) have been explored numerically and analytically quite thoroughly although still incompletely up to now; see for example [1,4]. In particular it was reliably established that the boundary of stochastic motion lies at $K = 1$ with an accuracy on the order of several percent. It follows from this that the width of a stochastic layer ($|y| < y_m$) is approximately equal to

$$y_m \approx \lambda;\ w_m \approx \lambda\xi\ ; \tag{2.2}$$

i.e., $\lambda = \Omega/\Omega_\phi = \Omega/\sqrt{\varepsilon}$ times larger than the splitting of the separatrix. With an additional condition $\eta << \varepsilon$ the accuracy of the last estimate $\delta y_m/y_m \sim 1/\lambda$ is essentially determined by the location of the extreme resonance with $y_r \approx \lambda$ [1]. In the case of $\eta \gtrsim \varepsilon$, the assessment (2.2) is correct only within an order of magnitude [1] as are all earlier estimates of the stochastic layer width (see for example [5-7]). Note that for $\eta \gtrsim \varepsilon\lambda/\nu 2$, the configuration of the stochastic layer significantly changes because of the appearance of a stable region in the neighborhood of $\phi = 0$ due to dynamic focusing which exists till $\eta \lesssim \varepsilon\lambda^2/\nu^2$.

The stochastic layer in the separatrix region of nonlinear resonance remains for any small perturbation ($\varepsilon \to 0$), although its width decreases

exponentially (1.3). The significance of such a stochastic component consists in that, with a many-dimensional system (with a number of degrees of freedom $n > 2$), the stochastic layers of nonlinear resonances intersect each other and form a system of channels in which a trajectory can travel any distance from its initial position. This process is known as Arnold diffusion and it was already discussed in one of the international conferences on nonlinear oscillations [8] (see also [1,9,10]). Arnold diffusion turns out to be a universal stochastic instability in many-dimensional Hamiltonian systems [1]. At the same time, the stochastic layer of nonlinear resonances acts as a "seed" for significantly stronger and more dangerous global stochastic instability, which arises with the increase of the width of the resonances and of their stochastic layers with increasing perturbation and their merging into a continuous stochastic component.

3. Global Structure of a Stochastic Layer

According to [1] a stochastic layer of nonlinear resonance can be roughly divided into two parts:

1. The central part $|y| \lesssim y_m/4$ (2.2) where apparently a stable component is completely absent (see also [11]) or, in any case, plays a very small role.

2. The peripheral parts ($y_m/4 \lesssim |y| < y_m$) where a significant stable component with a very complex hierarchical structure is present (see [1] and section 4 below). It is precisely in this peripheral region that the main difficulties of studying the motions in the stochastic layer are found.

Figure 1 illustrates an equilibrium distribution function in a layer $f_o(y/\lambda)$ averaged with respect to phase θ. The equilibrium distribution is obtained for one trajectory after $T = 10^7$ iterations of mapping (1.4), the dimension of one cell of the histogram was $\Delta(y/\lambda) = 10^{-2}$ and $\lambda = 9$. Figure 1 clearly shows that in the region $|y/\lambda| \lesssim 0.4$, the distribution function is practically constant $f_o(y/\lambda) = 1.1$. A small deviation from the value of f_o is found at the level of statistical fluctuations. For $|y/\lambda| \gtrsim 0.4$ the function $f_o(y/\lambda)$ decreases while in the interval $0.5 \lesssim |y/\lambda| < y_m/\lambda = 1.18$, the equilibrium function can be described on the average by the empirical formula (see Figs. 1 and 2):

$$f_o(x) = Cx^{\delta}; \quad x = \frac{y_m - |y|}{\lambda} \quad . \tag{3.1}$$

A least squares fit gives $\langle \log C \rangle = 0.089$ and $\langle \delta \rangle = 0.48 \approx 1/2$. Figure 2 presents the function $f_o(x)$ in the peripheral portion of the layer. The straight line corresponds to the equations (3.1) for $\delta = 1/2$ and $C = 1.2$. Oscillations of f_o are determined by system resonances (1.4) ($y_r = \exp(2\pi r/\lambda)$ and they depend on λ. However, the averaged distribution (3.1) apparently remains unchanged.

The crude properties of $f_o(x)$ can be explained on the basis of the following qualitative representations. The equilibrium density of stochastic trajectory in plane (y,θ) differs from zero and is constant only in the stochastic component, i.e., in the entire stochastic layer with the exception of stability islands ("holes"). The projection of the density on y axis

(averaging with respect to θ) will lower the distribution function $f_o(y/\lambda)$ in the hole region. A number of such dips are clearly seen in Fig. 1. Because a stable component is practically absent in the central portion of the layer, then in this region $f_o(y/\lambda) \approx$ const and in the peripheral portion, where the degree of component stability grows with the increase of y, f_o decreases.

Let us note that because of the changes in the distribution function [$f_o(y/\lambda) \neq$ const], the Fokker-Planck-Kolmogorov (FPK) equation describing the diffusion along y at $\lambda >> 1$, contains also a nondiffusion term [13]:

$$\frac{\partial f}{\partial t} = - \frac{\partial q}{\partial y} ; \quad q = D(y) \frac{\partial f}{\partial y} + Q(y) f . \tag{3.2}$$

The function Q(y) can be expressed through $f_o(y)$ [12]: $Q(y) = (D/f_o)(df_o/d_y)$. In our case it follows from the equilibrium property of the distribution function f_o that $Q = 0$ in the central portion of the stochastic layer, while in the peripheral region

$$Q = - \frac{\lambda D \ \mathrm{sgn}(y)}{2(y_m - |y|)} \tag{3.3}$$

[see (3.1)]. It must be noted that for $Q \neq 0$ detailed equilibrium is disrupted, i.e., probabilities of forward and return passes are not equal. This is caused by the presence of stable regions in the peripheral portion of the layer and which causes the fraction of the stochastic component in the interval dy to depend on y. If a new "equilibrium" variable is introduced

$\mu = \int_o^y f_o(y')\ dy'$ which is simply a normalized degree of a stochastic component, then the flux q becomes purely diffusive [$Q \sim df(\mu)/d\mu = 0$]. In the variable μ, the detailed equilibrium is re-established and the FPK equation assumes a simple form

$$\frac{\partial f(\mu,t)}{\partial t} = \frac{\partial}{\partial \mu}\left(D(\mu)\ \frac{\partial f(\mu,t)}{\partial \mu}\right) \tag{3.4}$$

$$D(\mu) = D(y)\ \left(\frac{d\mu}{dy}\right)^2 = D(y)\ f_o^2\ (y)\quad .$$

For more details see [13].

4. Peripheral Portion of a Stochastic Layer

We will use Poincaré statistics of returns to further investigate the structure of the peripheral portion of a stochastic layer.* This method was suggested by Ref. [14] which treated practically the same problem, although the authors do not mention it directly. The method consists of a numerical determination of the distribution of recurrence times (τ) of a trajectory of the mapping (1.4) to return to the center of the stochastic layer ($y = 0$, θ arbitrary). To simplify the data processing a joint statistic of recurrences was examined in both halves of the stochastic layer ($y > 0$ and $y < 0$) in which the motion differed only by a shift in phase ($\theta \to \theta + \pi$). The recurrence time

---

*Let us note the quasiperiodicity of motion does not follow from Poincaré recurrence theorem as it is sometimes assumed. In the present case, for instance, the spectrum of the motion is continuous.

was taken as equal to the full number of mapping iterations (1.4) between the two successive passes through the layer center $y = 0$. The integral distribution function $F(\tau)$ was determined from a single trajectory as a ratio of the number of recurrences N_τ with time $> \tau$ to the total number of recurrences N_o during the total motion time T.

A histogram of the distribution $F(\tau)$ for $\lambda = 1, 3, 5, 7, 10, 30, 100$ with $T = 10^7$ is shown in Fig. 3. It is seen that for sufficiently small $\tau < \tau_o(\lambda)$ the distribution $F(\tau)$ can be well described by the function $1/\sqrt{\tau}$ ($\tau > 1$) (straight line in Fig. 3) in agreement with results in [14]. However, for larger τ, the function $F(\tau)$ decreases at a more rapid rate and can be roughly approximated by the expression

$$F(\tau) \approx \frac{A(\lambda)}{\tau^p} ; \quad \tau >> \tau_o(\lambda) . \tag{4.1}$$

The average value from all the numerical data gives $\langle p \rangle = 1.45 \pm 0.05 \approx 3/2$, although individual p values are noticeably different, particularly for $\lambda = 1$ (1.64); $\lambda = 30$ (1.26); $\lambda = 100$ (1.27). The empirical dependence $A(\lambda)$ is shown in Fig. 4 and it can be described by $A(\lambda) \approx 3.5\lambda$ (straight line in Fig. 4). It must be mentioned that the actual distribution is significantly more complex than (4.1) and in particular, curves for different λ intersect at several points (Fig. 3) as though they were drawn together. A small plateau at the very end of some curves is due to low statistics ($N_\tau \sim 1$).

The initial dependence $F(\tau) \approx 1/\sqrt{\tau}$ is simply explained by the free diffusion at the central layer before the final layer width is reached (see for example [15]), i.e., for $\tau \lesssim \lambda^2$. In fact, numerical data show that the

boundary of the region is $\tau_o \approx 0.3\ \lambda^2$. If the relationship $F = 1/\sqrt{\tau}$ is preserved for all τ, then the average $\langle\tau\rangle$ would diverge [14]. However, for $\tau >> \tau_o$ the exponent $p > 1$, so that $\langle\tau\rangle$ is finite: $\langle\tau\rangle \sim -\int_o^{\tau_o} F'(\tau)\ \tau\ d\tau = \sqrt{\tau_o} \sim \lambda$. Numerical experiments give $\langle\tau\rangle \approx 3.2\lambda$ (with the exception of when $\lambda = 1$).

Let us note that although $\langle\tau\rangle$ is finite, $\langle\tau^2\rangle$ diverges for $p = 3/2$. This increases the fluctuations which were apparently observed in [14]. For example, the fluctuations of the numerical value $\langle\tau\rangle$ along a single trajectory are

$$\frac{\langle\tau^2\rangle - \langle\tau\rangle^2}{N_o\langle\tau\rangle^2} \sim \frac{3}{T^{2/3}}\left(\frac{A}{\langle\tau\rangle}\right)^{4/3} . \qquad (4.2)$$

Let us explain that the decrease in fluctuations with T is related to the fact that $\langle\tau^2\rangle \propto \sqrt{\tau_m} \propto N_o^{1/3}$ increases slower than N_o. The maximum growth time τ_m is found from the condition $F(\tau_m) \sim N_o^{-1}$. The estimate (4.2) is confirmed by numerical data.

The distribution shape $F(\tau)$ makes possible certain considerations about the structure of the stochastic layer. In particular, it is possible to attempt to relate dependence (4.1) to the diffusion speed near the edge of a stochastic layer.

Local properties of mapping (1.4) and in particular the diffusion coefficient along y are characterized by the parameter $K = \lambda/y \approx 1/(1-x)$ [see (2.1)], which depends only on x. Let us assume that $x \to 0$, $D_y(x) = D_x(x)\lambda^2 \sim x^\alpha$, so that the diffusion speed drops toward the edge of the layer. It is then possible to accept, as a first rough approximation, that

the return time τ (for $\tau \to \infty$) is found to be, within an order of magnitude, the average diffusion time from the region $x \to 0$ to the center of the layer. This is $\tau \sim x^2/D_x \sim \lambda^2 x^{2-\alpha}$. Thus the recurrence with time $> \tau$ are related to the entry of the trajectory into the region $x \lesssim (\lambda^2/\tau)^{1/(\alpha-2)}$. On the other hand, the extent of this region is related to the distribution $F(\tau)$ by means of

$$\mu(x) \sim \frac{N_\tau \tau(x)}{T} \sim \frac{N_\tau \tau}{N_o \langle\tau\rangle} = \frac{F_\tau \tau}{\langle\tau\rangle} \qquad (4.3)$$

as result of ergodic motion. The function $\mu(x)$ is obtained from (3.1)

$$\mu(x) = \int_o^x f_o(x)\, dx \sim x^{1+\delta} \quad .$$

We finally find (for $\alpha > 2$)

$$F(\tau) \sim \frac{\lambda^\kappa}{\tau^p} \; ; \; p = 1 + \frac{1+\delta}{\alpha - 2} \; ; \; \kappa = 2p - 1 \; . \qquad (4.4)$$

I.e., the distribution $F(\tau)$ at $\tau \to \infty$ is a power function and not exponential as it is usually considered (see for example [14]). This is related to the fact that for $\alpha > 2$ the trajectory does not reach the edge of the layer ($x = 0$) during a finite time. For $\alpha < 2$ the diffusion time across the layer is finite and then, as it is known, the distribution $F(\tau)$ decreases exponentially due to diffusion statistics. It is possible to show that at

$\alpha = 2$ the function $F(\tau)$ is also exponential, although the average diffusion time from the layer edge is infinite.

Using the empirical expressions mentioned above $p = 3/2$, $\delta = 1/2$, we find that $\alpha = 5$, $\kappa = 2$. The value of α exceeds significantly the value $\alpha \approx 2.6$ found in [1] by direct measurements of diffusion speed, however, large fluctuations make this value unreliable. On the other hand, the value $\delta = 1/2$ cannot be considered as final, particularly for $x \to 0$. In addition, it is possible to conclude from the data of [1] that $f_o(x) \to 0.5$ for $x \to 0$. This does not contradict Fig. 1, with the exception of the region $|y/\lambda| > 1.1$ where the function $f_o(x) \sim \sqrt{x}$ can be explained, for example, by the curvature of the layer edge. Then $\delta = 0$ and $\alpha = 4$.

The value $\kappa = 2$ differs from the empirical $\kappa = 1$, although this difference cannot be considered firmly established because of points scatter in Fig. 4. Furthermore, if we neglect cases where $\lambda = 1$ (too few) and $\lambda = 30$, 100 [insufficient count time for asymptotic exit (4.1)], then the four remaining cases give $A = \lambda^{1.76}$. This problem therefore requires further study.

In spite of a certain indeterminacy in the numerical results and the calculations, it can be considered established, it appears to us, that the statistics of trajectory recurrence times into the stochastic layer decrease nonexponentially. This result apparently remains correct also for two other boundary types between stochastic and stable components. In particular, the numerical experiments presented by us with mapping (1.4) substituting $\lambda^2/|y|$ for $\lambda \ln|y|$ show that the distribution $F(\tau)$ has the form (4.1) with exponent $\langle p \rangle = 1.71 \pm 0.11$.

REFERENCES

[1] B.V. Chirikov, Physics Reports 52 (1972) 263.

[2] N.N. Bogolybuov, Yu. A. Mitropol'sky, "Asymptotic Methods in the Theory of Nonlinear Oscillations," Hindustan Publ. Corp., Dehli, 1961.

[3] Y.K. Mel'nikov, Dokl. Akad. Nauk USSR 142: 3 (1962) 542. Proc. of Moscow Math. Society, 12 (1963) 3.

[4] J.M. Greene, J. Math. Phys. 20 (1979) 1183.

[5] G.M. Zaslavsky, N.N. Filonenko, Zh. Exper. Teor. Fiz. 54 (1968) 1590 (Sov. Phys. JETP 27 (1968) 851).

[6] B.V. Chirikov, "Investigations of Nonlinear Resonance Theory and Stochasticity," preprint 267, Institute of Nuclear Physics, Novosibirsk 1969.

[7] A.B. Rechester, T.H. Stix, Phys. Rev. Lett. 36 (1976) 537.

[8] G.V. Gadiyak, F.M. Izraylev, B.V. Chirikov, Proc. of 7th International Conference on Nonlinear Oscillations (Berlin 1975), Vol. II, 1, p. 315.

[9] J.L. Tennyson, M.A. Lieberman, A.J. Lichtenberg in Nuclear Dynamics and the Beam-Beam Interaction, A.I.P. Conf. Proc. No. 57, (1979), p. 272.

[10] B.V. Chirikov, J. Ford, F. Vivaldi, ibid, p. 323.

[11] A.J. Lichtenberg, M.A. Lieberman, R.H. Cohen, "Fermi Acceleration Revisited," preprint UCB/ERL M80/36, College of Engineering, University of California, Berkeley, 1980.

[12] E.M. Lifshitz, L.P. Pitaevsky, Physical Kinetics, Nauka, M. 1979.

[13] B.V. Chirikov, D.L. Shepelyansky. "Diffusion with Multiple Passages of Nonlinear Resonance," preprint 80-211, Institute of Nuclear Physics, Novosibirsk, 1980.

[14] S.R. Channon, J.L. Lebowitz, "Numerical Experiments in Stochastic and Heteroclinic Oscillation," Annals of the New York Academy of Sciences 357 (1980) 108.

[15] A.A. Borovkov, "Theory of Probability," Nauka, M. (1976).

Figure Captions

Fig. 1 Equilibrium distribution function in a stochastic layer for $\lambda = 9$; broken line - 10^7 iterations; circles - 4×10^6; curve (3.12) with $\delta = 1/2$, $C = 1.3$.

Fig. 2 Same as in Fig. 1, but at a different scale, straight line corresponds to the curve of Fig. 1. Logarithms here and further on have a decimal base.

Fig. 3 Distribution of trajectory recurrences in a stochastic layer; $\lambda = 1$ (+), 3 (•), 5 (0), 7 (*), 10 (×), 30 (Δ), 100 ([ ]), straight line - $F(t) = 1/\sqrt{\tau}$.

Fig. 4 Function $A(\lambda)$, dots - numerical count, straight line - matching ($A = 3.5\lambda^{1.06}$).

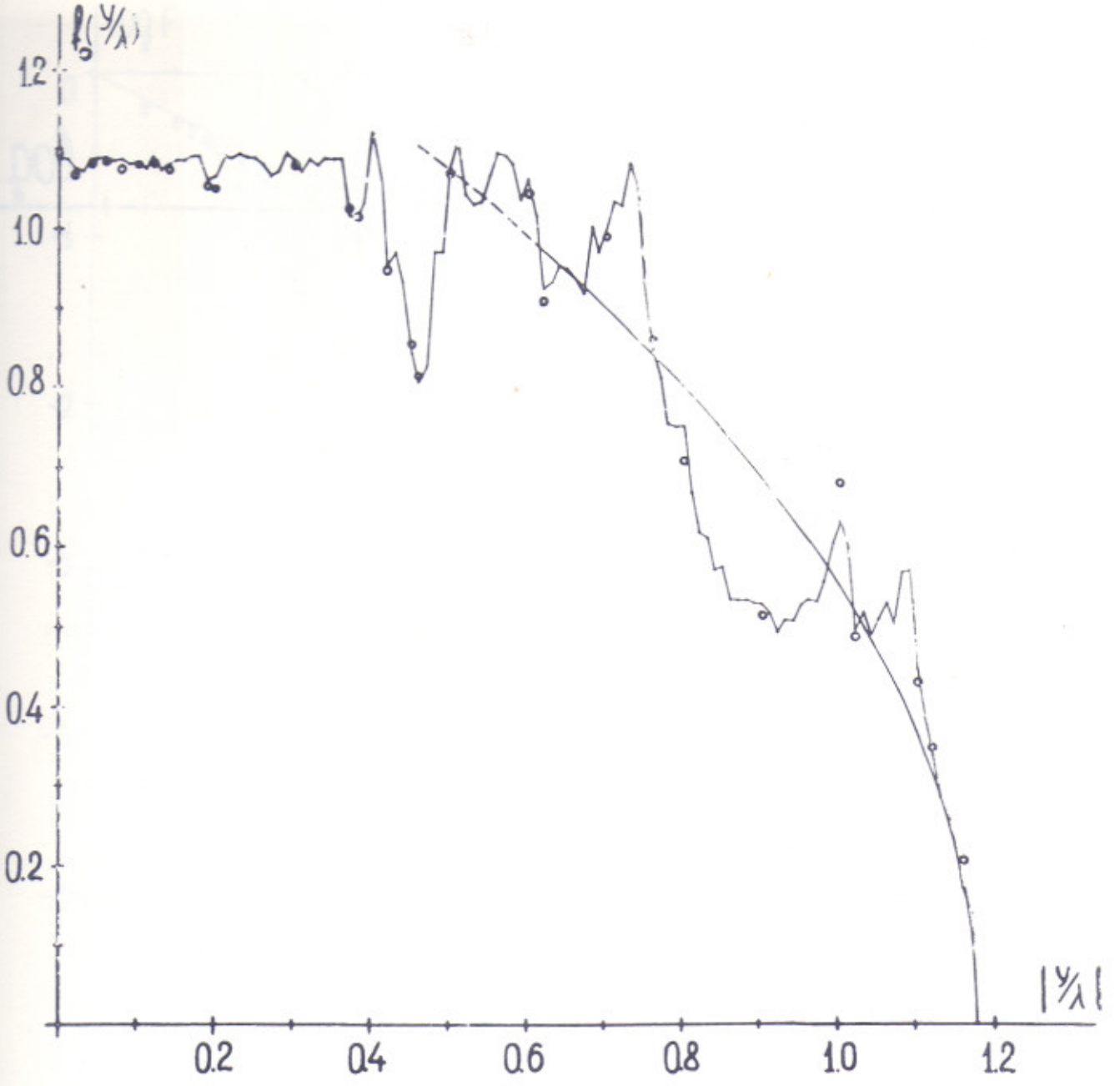

Fig. 1

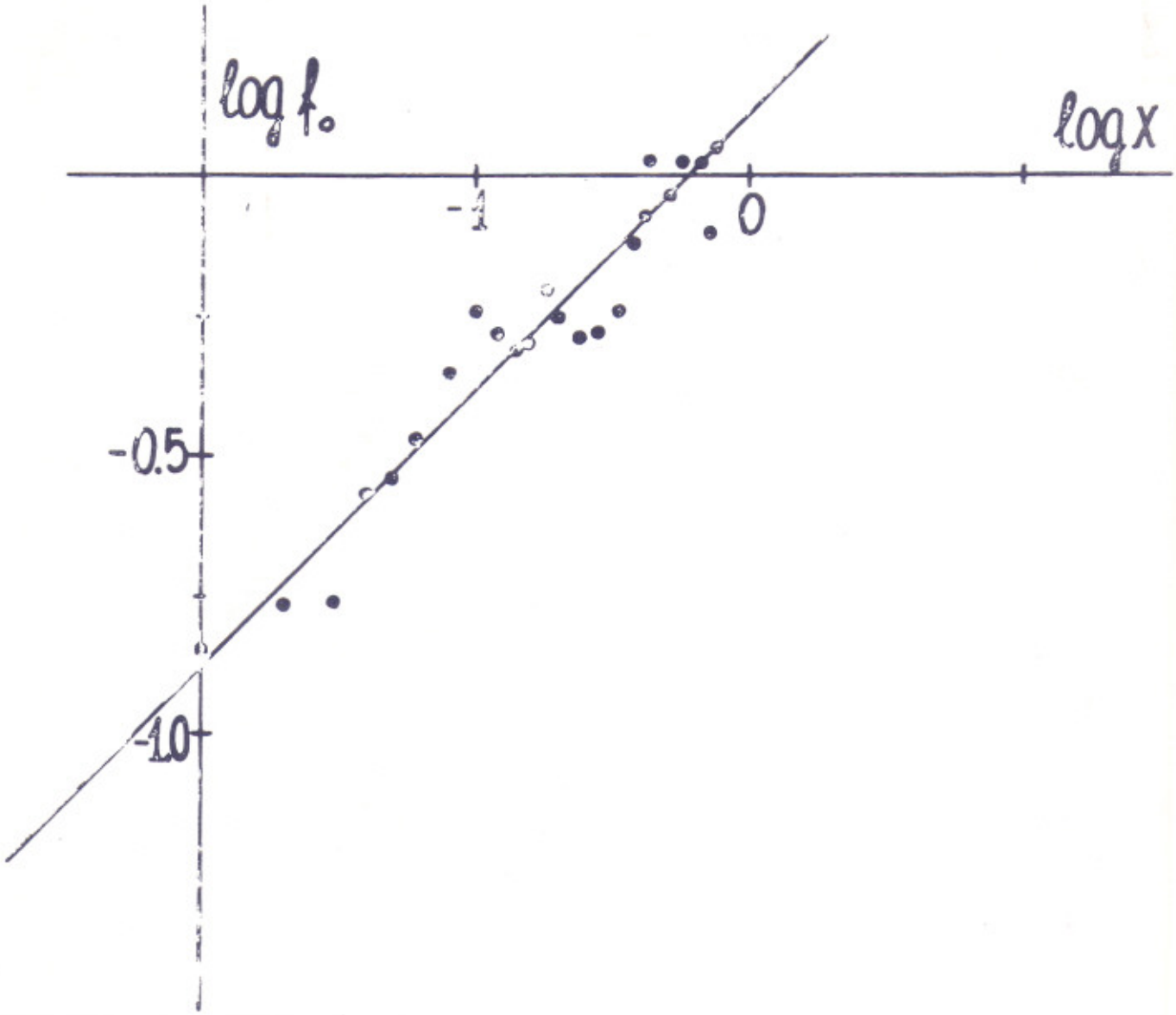

Fig. 2

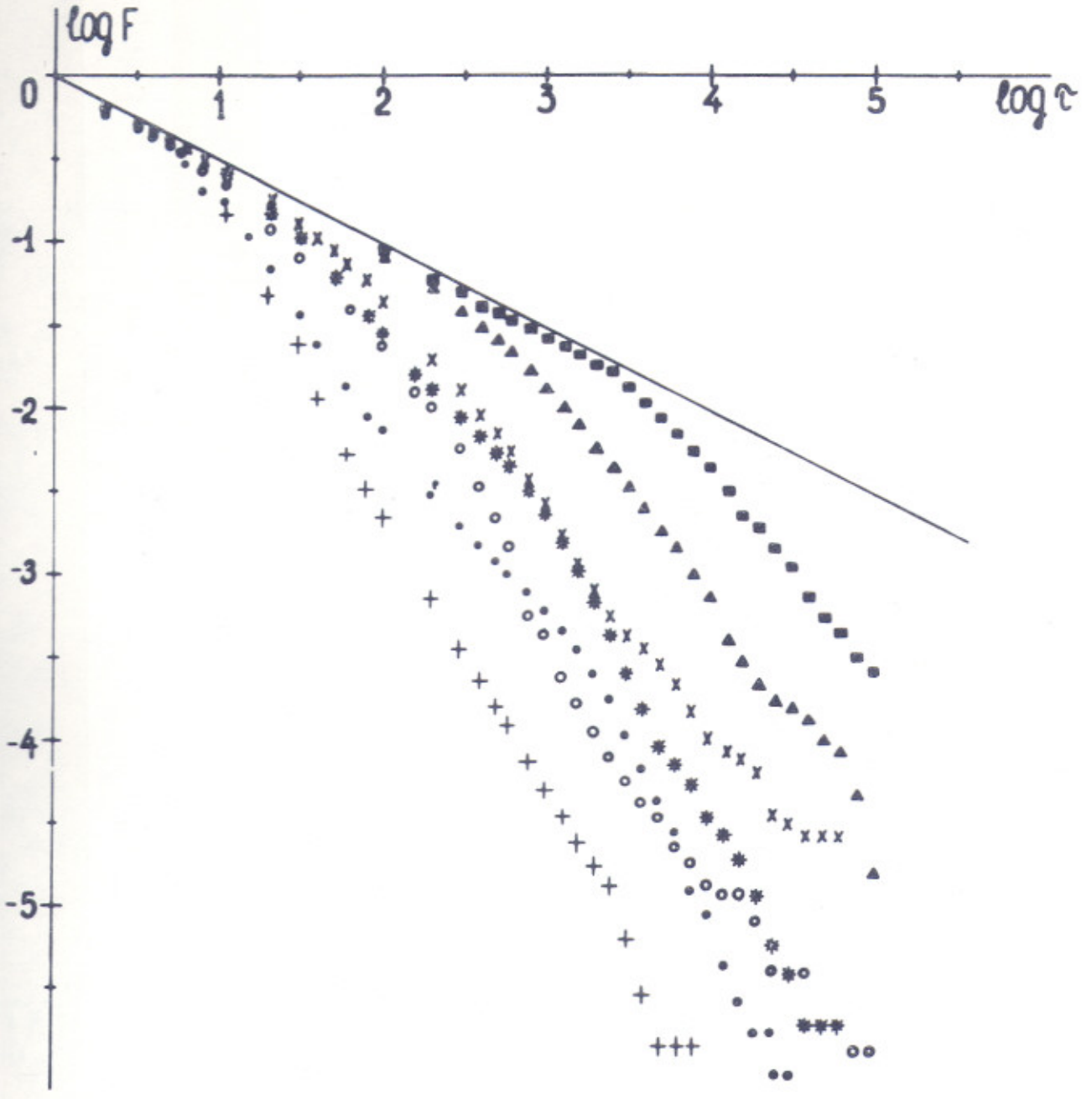

Fig. 3

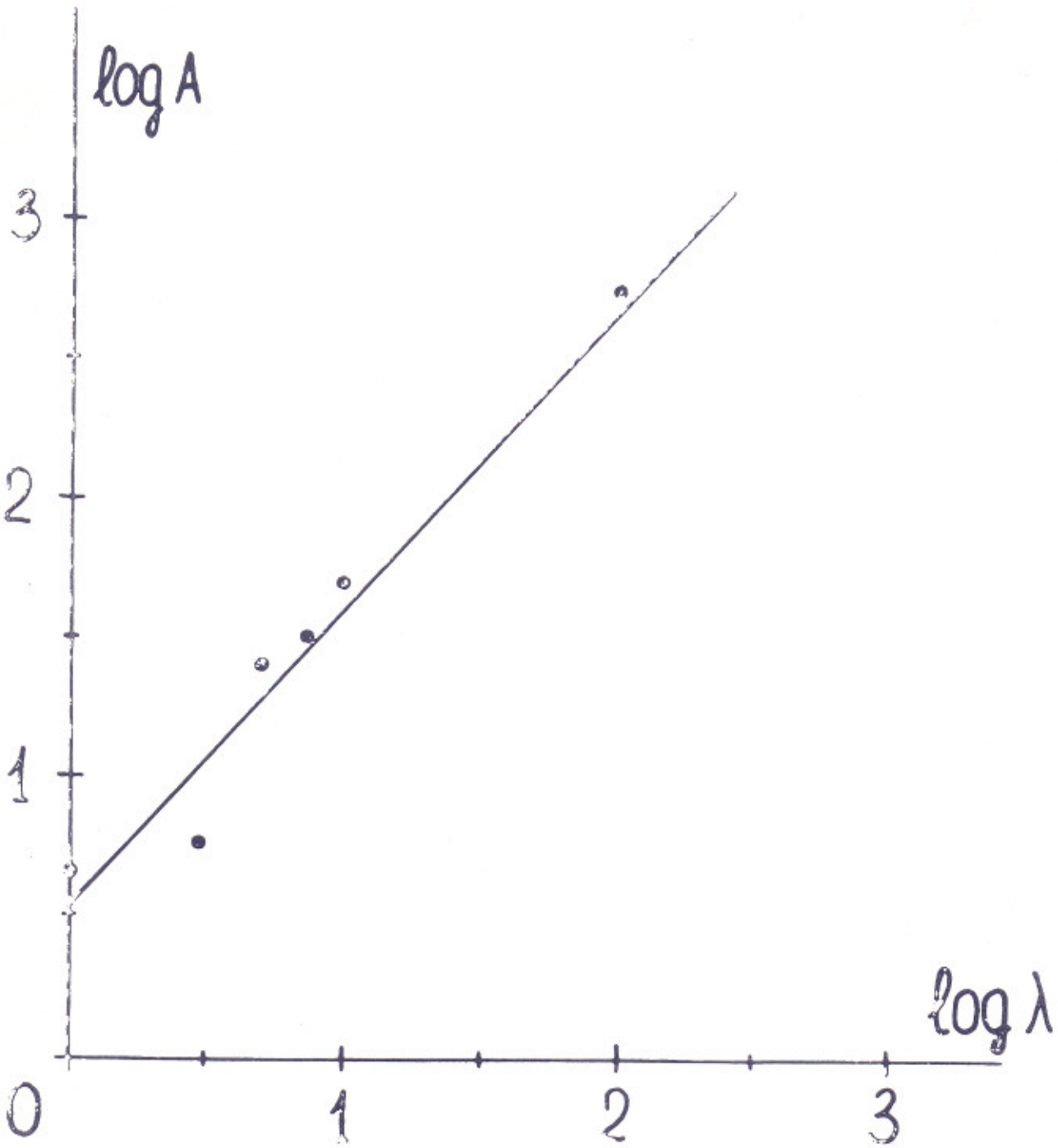

Fig. 4